

Development and testing of vertical take-off and landing aerial vehicle with tandem electric ducted fan motor

Kristjan Pütsep*, Tõivo Nerep, Hans Tiismus and Anton Rassõlkin

Department of Electrical Power Engineering and Mechatronics, Tallinn University of Technology, Ehitajate tee 5, 19086 Tallinn, Estonia

Received 24 January 2023, accepted 2 March 2023, available online 2 May 2023

© 2023 Authors. This is an Open Access article distributed under the terms and conditions of the Creative Commons Attribution 4.0 International License CC BY 4.0 (<http://creativecommons.org/licenses/by/4.0>).

Abstract. Due to the complexity of control mechanisms, vertical take-off and landing (VTOL) aerial vehicles have not found their way into widespread commercial use. Thanks to the availability of advanced technology, it is possible to develop simpler systems. Such systems could be used in transportation, the military, surveillance, etc. The research work is aimed at proposing an automatic stabilisation control algorithm solution for the VTOL hover flight phase. A critical analysis of the existing research work on a similar topic is provided. A flight platform and a suitable test bench for non-destructive tests were developed and presented in the current paper. The flight platform actuator system consists of two counter-rotating electric ducted fan (EDF) thrust motors and two servo systems that control pitch and roll movements. Moreover, the paper presents control algorithm development, structure, and experiments that confirm the proposed solutions. The results of the research work provide a solid foundation for developing the VTOL aerial vehicle, and the test bench prototype demonstrates a concept that can be further used on various flight platforms.

Keywords: unmanned aerial vehicles, system testing, motors.

1. INTRODUCTION

In general, aerial vehicles can be divided into two categories: fixed-wing and rotary-wing, both having advantages and disadvantages. The aerodynamics of traditional fixed-wing aerial vehicles is presented in [1], and conventional rotary-wing aerial vehicles in [2–4]. Regarding the aerodynamics of the object, it is affected by two main forces: lift and drag. The lift acts perpendicular to the relative wind and opposes another force called weight. Drag is parallel to the relative wind and opposes the force called thrust. The operation of fixed-wing aerial vehicles depends on the availability of a sufficient runway for take-off, which leads to a critical selection of the site. On the other hand, the flight range of such a platform is significantly longer than rotary-wing aerial vehicles can provide. In [3,4], more detailed studies regarding the aerodynamics affecting rotary-wing aerial

vehicles are provided. Rotary-wing aerial vehicles can take off vertically and hover but have higher power consumption. In [1], detailed studies regarding fixed-wing aerial vehicles' aerodynamic effects are discussed.

Due to both disadvantages, research society has been exploring the possibilities of figuring out a hybrid version that can take off vertically, hover, and transit into a more economical forward flight. Those systems are called vertical take-off and landing (VTOL) aerial vehicles. The first known VTOL aircraft made its first flight in 1954 [5]. A single unit was produced and the project was canceled in 1955. The aircraft could fly, but it was considered too dangerous since the pilot had poor visibility during vertical take-off and landing. Furthermore, the VTOL aerial vehicles were primarily developed with a design where not the aircraft itself was tilted to achieve translational flight, but instead, motors and wings were tilted or engine airflow deflected downwards. Such aerial vehicles have complex and challenging control logic and moving mechanical systems.

* Corresponding author, kristjan.pytsep@taltech.ee



Fig. 1. Design examples of (a) tail-sitter [8], (b) tiltrotor [9], and (c) tiltwing [10] vertical take-off and landing (VTOL) aerial vehicles.

G. Ducard and M. Allenspach [6] analyse different VTOL concepts and share know-how on the VTOL aerial vehicle control system development. First of all, the authors give a historical overview of manned and unmanned VTOL configurations and summarise that the most well-known manned VTOL designs have been developed for military purposes. However, the developed systems did not meet expectations and the number of successful flights was limited. At the same time, unmanned VTOL designs have been more successful, although only a few have been completed. The design of most projects is complex and leads to costly maintenance.

Y. Zhou et al. [7] describe a similar view of conceptual classification. Unmanned VTOL aerial vehicles are divided into three categories: tail-sitter, tiltrotor, and tiltwing (as shown in Fig. 1). The tail-sitter concept (Fig. 1a) contributes to a simple mechanical design, where rotors are attached rigidly to the fuselage. To obtain hover flight, the whole aircraft is tilted. However, this design is more complex to control in comparison to the others due to the tilt of the entire aircraft, and a large wing area is exposed to winds during the hover phase. This will generate significant disturbances that actuators try to compensate for, leading to power loss due to the stabilisation process. The tiltrotor concept (Fig. 1b) maintains fuselage orientation regardless of the flight phase. This was realized by tilting only the rotors to obtain hover flight. The major disadvantage here is that part of the wing will be in propeller downwash during hover flight, which reduces potential propeller capability. The tiltwing concept (Fig. 1c) maintains its fuselage similarly to the tiltrotor concept (Fig. 1b), but the rotors are rigidly attached to the wing and the entire wing is tilted. Such design allows using potential propeller capability to a greater extent. Moreover, flight controls will be rotated together with wings, making it possible to use them in hover flight. This concept has a complex wing-tilting mechanism and deadweight associated with it.

Barth et al. [11] compare model-based and model-free control approaches of the tail-sitter VTOL aerial vehicles. The authors have found that a model-free controller can

better reject disturbances than a model-based controller. Bonci et al. [12] propose the concept of an unmanned aerial vehicle (UAV) to assist in automated maintenance procedures for infrastructure systems. The paper presents a concept of a double propeller ducted fan tail-sitter VTOL, which is highly similar to the concept under research in the current project. The authors describe a detailed dynamic model and propose a control solution, which is then validated with the aid of simulation. However, testing with a physical prototype is not included in [12]. The authors point out that counter-rotating propellers cancel out reaction pairs generated by the gyroscopic precession torque effect. Furthermore, this solution allows designing controls to solve yaw dynamics purely by using ducted fans. Several research works by Naldi et al. [13–15] cover similar projects, where a solution is sought for the VTOL concept powered by a ducted fan, which uses a single propeller design. This leads to higher actuation expectations for other flight controllers to overcome rotational momentum generated by a single thrust propeller.

In [16], Zhang et al. have constructed a novel tandem ducted fan vehicle, which is not intended to be the VTOL aerial vehicle, but uses two thrust engines with counter-rotating and axially positioned propellers. The research includes nonlinear modeling, attitude control system design, and simulations. In conclusion, the authors stated that additional speed and position control research must be carried out with various flight experiments.

Literature review reveals numerous papers dedicated to controlling the design and simulation of the VTOL aircraft. Many authors have acknowledged that accurate dynamic models are too complex for realistic simulations. None of the existing research papers have offered a solution for VTOL with a tandem electric ducted fan (EDF) motor. This work focuses on an innovative solution that makes a simple and robust control design possible.

EDFs are known as powerful motors with high energy consumption. Integrating two counter-rotating EDF motors into one tandem engine provides a powerful thrust system with specific benefits compared to the conventional pro-

PELLER. According to M. Lihulinn [17], the advantages of EDFs are as follows: smaller dimensions, higher thrust, higher ventilator efficiency factor at higher flight speeds, higher static thrust at smaller dimensions of the propeller, lower noise level, safer operation due to lack of exposed propellers, good prerequisites to use in VTOL applications, and higher exhaust airflow speed. However, there are several disadvantages of EDFs such as vortex footprint (generated by the high rotational speed), angular momentum (generated by an electrical motor), high energy consumption, complex profile of the surrounding housing generating parasite drag, and lower efficiency at low speeds.

This review of the existing research has revealed that the topic needs further development and analytical data from tests carried out in a physical environment. Most existing papers use simplified dynamic models and validate solutions only in simulation. The conclusion of the reviewed literature is provided in Appendix.

The research gap is that a dynamic model for such a concept is highly complex for precise calculation. On the other hand, there already exist analyzed dynamical models and promising results validated in simulators. Therefore, this paper concentrates on the following aspects: constructing an unmanned VTOL tail-sitter, constructing a test bench for non-destructive testing, proposing a control solution with the dedicated algorithm on an embedded system platform, and validating solutions in a realistic environment (avoiding dynamic model calculations and simulations).

2. VTOL CONSTRUCTION AND DESIGN PROCESS

2.1. Flying platform

The design concept of the basic tail-sitter is first compiled into a 3D model for verification and use in the additive manufacturing process. The research is focused on the design for a stable hover flight; therefore, the design of wings is not presented. Fuselage components are manufactured using 3D printing technology. Figure 2 shows an overall model with the coordinate system. Dynamics regarding coordinates are as follows: rotation around y – roll axis, around x – pitch axis, around z – yaw axis.

The tandem EDF motor assembly responsible for generating lift force and controlling yaw angle is presented in Fig. 3. The assembly consists of nine items, most of which are the original parts from Dr. Mad Thrust 70 mm EDF motor [18]. The completed thrust motor is a counter-rotating tandem EDF motor. This assembly is responsible for generating lift force and controlling yaw angle.

The roll and pitch control assembly design is presented in Fig. 4. Housing mounts all these parts together and

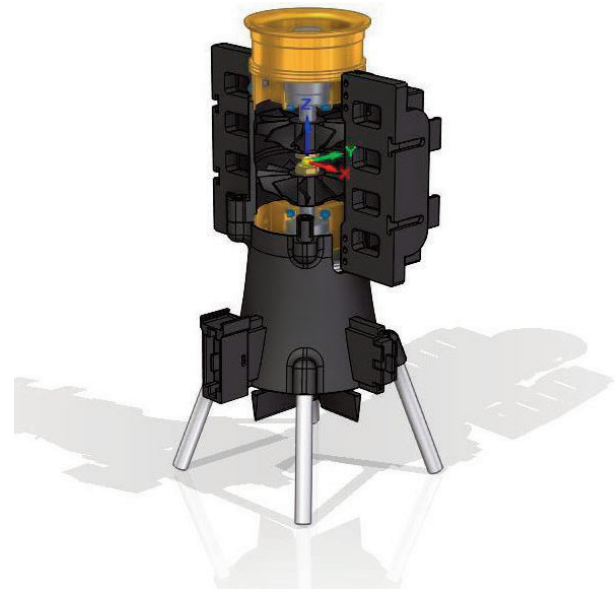


Fig. 2. 3D model of the developed tail-sitter platform with the cut view of engine section and coordinate system (around y – roll axis, around x – pitch axis, around z – yaw axis).

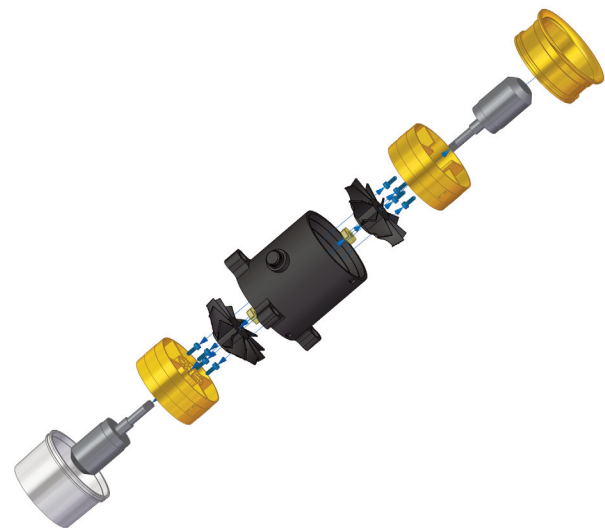


Fig. 3. Tandem electric ducted fan (EDF) motor assembly.

connects control frame assembly to tandem EDF motor assembly, and supports aluminum tubes acting as landing gear. Servo actuators are responsible for moving control surfaces, which are responsible for controlling roll and pitch angles.

The final subassembly of the fuselage is the battery compartment assembly in Fig. 5. The fuselage assembly consists of two battery compartments. Battery dimensions

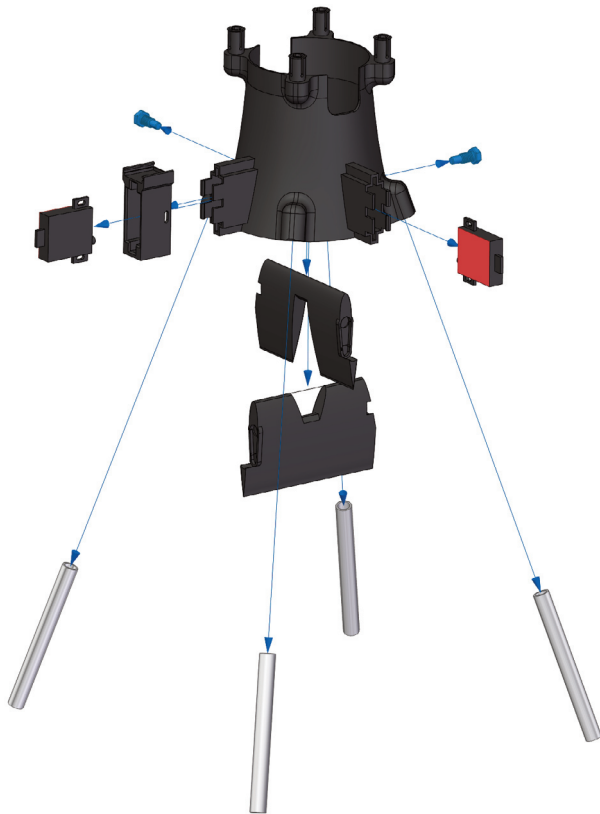


Fig. 4. Control frame assembly exploded view.

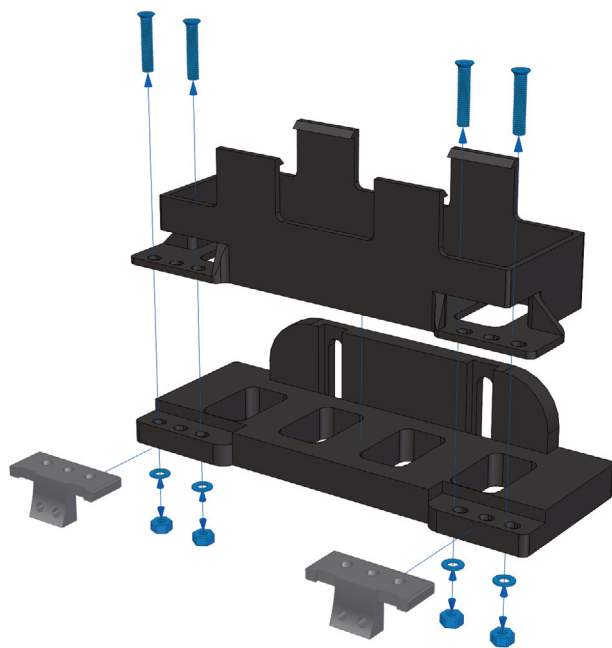


Fig. 5. Battery compartment assembly.

are the main design criteria for this subassembly as it needs to fit the battery inside the compartment.

2.2. Actuators

Thrust motors are a major part of any aerial vehicle, being the decisive factor to set the criteria for the other components. Dr. Mad Thrust 70 mm 10 blade Alloy EDF 3000 Kv [18] motors were chosen for good quality and high performance, based on the research team experience. Specifications of the selected motor are shown in Table 1: dimensions set the fuselage design criteria, motor type defines maximum speed, and that in turn defines maximum voltage. A simplified relation between them is shown in Eq. 1. Considering the motor’s type, maximum speed, maximum voltage and power ratings, batteries and electrical speed controllers (ESC) were chosen:

$$\omega = Kv \cdot V_{max}, \tag{1}$$

where: ω – maximum motor speed (RPM),

Kv – constant velocity of a motor that represents the number of revolutions per minute (rpm) that a motor achieves when 1 V is applied to the motor terminals with no load attached to that motor [19],

V_{max} – maximum voltage (V).

To estimate the actual rotational speed, the batteries’ charge level (fully charged 4s LiPo battery voltage is 16.8 V) and load on the motor must be taken into account. Therefore, the values in Table 1 do not exactly correspond to the values resulting in the calculation.

The ESC decision is important to get the best possible motor performance. For that reason, hardware components

Table 1. EDF motor specifications [18]

No.	Parameter	Value
1.	EDF inner diameter [mm]	69.00
2.	EDF outer diameter [mm]	72.00
3.	Number of blades	10.00
4.	Maximum speed [RPM]	48 000.00
5.	Constant velocity [Kv]	3000.00
6.	Continuous power [W]	1200.00
7.	Maximum voltage [V]	14.80
8.	Maximum current [A]	83.00
9.	Maximum thrust [g]	2300.00
10.	Weight [g]	256.00

were ordered from the same retailer to simplify logistics. BEC (battery elimination circuit) characteristics are not considered relevant during the decision making as a solution has its voltage regulator and power distribution circuit. The chosen product is HobbyKing 80A (2 – 6S) ESC 4A SBEC speed controller.

Control surface servo actuators are difficult to select prior to the design and testing phase. A rotational range of 180 deg is sufficient for servo application in this project. Corona CS – 239MG was chosen for that purpose.

2.3. Power distribution

Servo actuators, microcontrollers, and sensors are powered with low voltage (5 V), and EDF motors and ESCs are powered with high voltage (14.8 V). Based on that, a power distribution circuit was constructed. The power distribution circuit ensures sufficient voltage and current for the components. If the flight platform is further developed into a horizontal flight-capable VTOL, the control surfaces are expected to remain functional in the event of ESC failure. For this purpose, an independent voltage regulator board was used.

Two batteries act as a power source. The decision for batteries was based on the EDF motor characteristics. The selected motors use a current up to 83 A at an input voltage of 14.8 V. This means that a four-cell lithium polymer battery would be sufficient. It also defines maximum load conditions and sets criteria for the battery C-rating, which indicates how fast the battery can be safely discharged. The chosen batteries are Turnigy 2.2 Ah 60 – 120 °C LiPo. A maximum discharge rate of 120 °C means that the whole battery capacity can be discharged within 30 seconds, which is calculated as follows:

$$t_{bat} = \frac{C_{bat}}{C_{rating} \cdot C_{bat}} \cdot 3600 = \frac{1}{C_{rating}} \cdot 3600, \quad (2)$$

where: t_{bat} – minimum time to discharge battery (s),

C_{bat} – battery capacity (Ah),

C_{rating} – battery C-rating.

Although the batteries can be discharged at a high rate, the powered time will be limited by their capacity. The following equation provides a calculation for the actual discharging time for maximum load conditions. This calculation indicates that even if one battery fails, the second battery can safely power both motors in maximum load conditions:

$$t_{min} = \frac{C_{bat}}{I_{EDF}} \cdot 3600, \quad (3)$$

where: t_{min} – minimum discharge time at maximum load(s),

I_{EDF} – EDF motor maximum current (A).

Calculations show that the chosen batteries can power motors in the case of maximum load for 95 seconds. However, it must be noted that calculations are made with maximum current conditions, and in the actual application, the highest currents may be drawn only in hover mode since during the horizontal flight phase (not tested in this paper) the current will decrease considerably.

2.4. Control boards

The overall design also contributes to its relatively small dimensions and weight. Control is provided by an embedded system, where a microcontroller performs controlling tasks. The inertial measurement unit (IMU) provides position feedback and acts as a sensor system. The system's heart is an Arduino Nano microcontroller and the sensing element is Adafruit BNO055 IMU. The Arduino Nano microcontroller is responsible for receiving information from the IMU sensor via I2C (Inter-Integrated Circuit) interface, calculating correct inputs and controlling the actuators. I2C is operating on standard mode (Sm), which allows communication speeds of up to 100kHz.

BNO055 processes and sends filtered data in quaternions, Euler angles or vectors [17]. Adafruit BNO055 absolute orientation sensor is used in the system, and it is based on ARM-Cortex-M0 microcontroller to process accelerometer, magnetometer, and gyroscope measurement data. The advantage over other similar sensors is that the data is already processed and ready for the host controller, reducing the load on the host and allowing it to focus on the primary control functions.

2.5. Flying platform

Most flying platform parts were produced using additive manufacturing. The overall printing time was 42 hours and 9 minutes, which did not include the design process and equipment preparation time or the failed attempts and repetitive prints due to the ongoing design development process. The final flying platform assembly is presented in Fig. 6.

An electrical circuit was completed to prepare a platform for algorithm implementation. The general block scheme of the control system is shown in Fig. 7., where the green lines represent PWM (pulse-width modulation) signal, the purple lines represent I2C, the red lines are battery voltage supply, and the blue lines are regulated supply connections.

Before constructing the aircraft, theoretical flight capability was assessed. For this purpose, all component weights were added together. The completed prototype's gross weight is 1760 g.

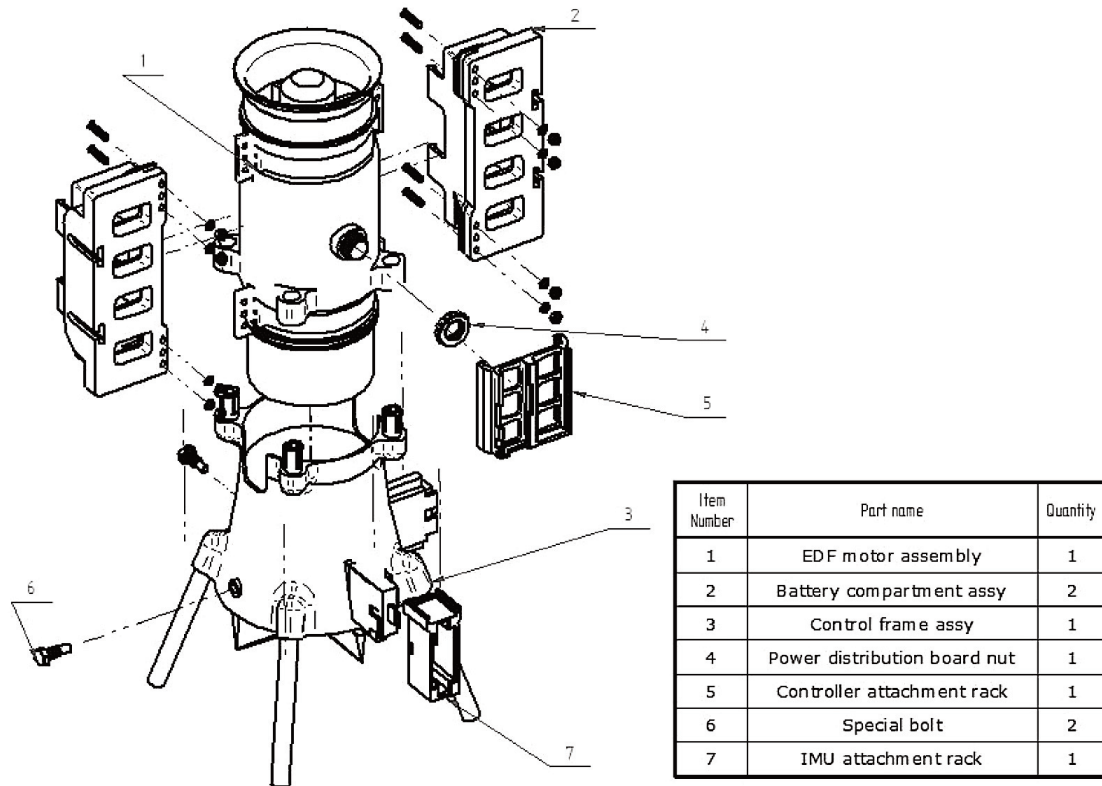


Fig. 6. Flying platform assembly.

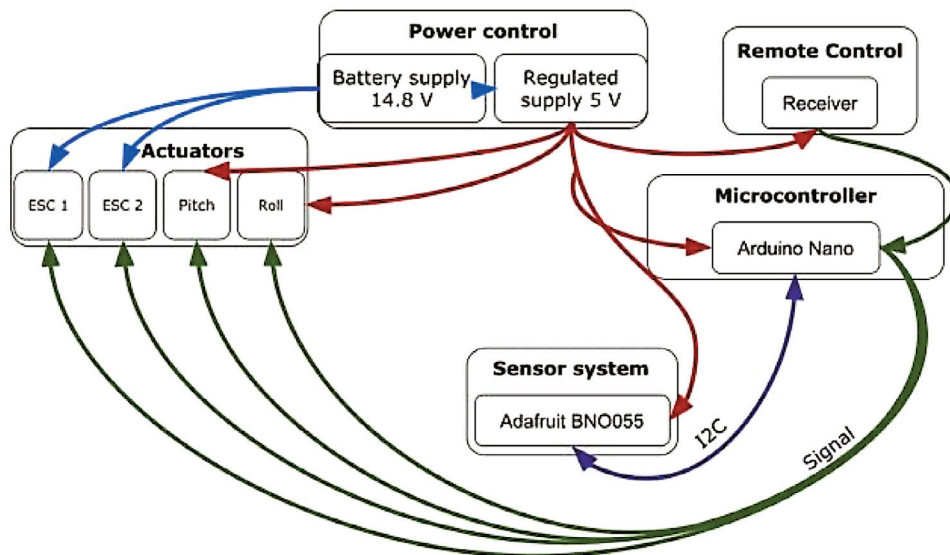


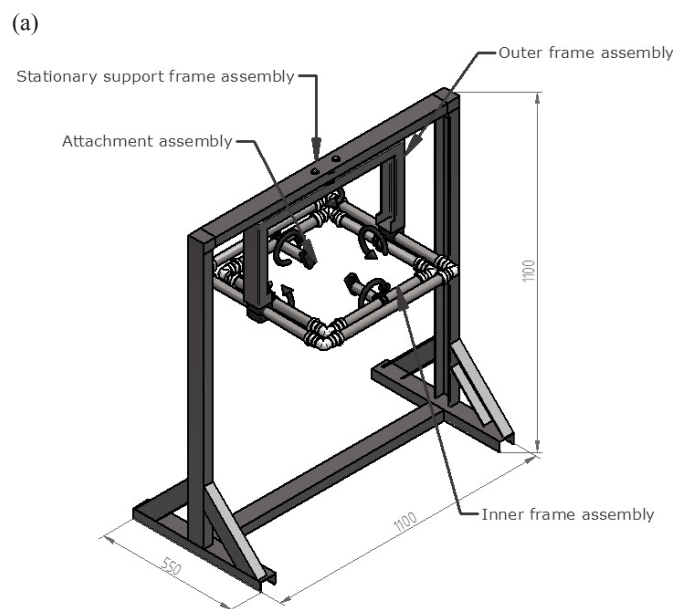
Fig. 7. Hardware connection block scheme.

3. EXPERIMENTAL PART

3.1. Test bench

Research has revealed that controllers can be tuned in different ways. For the current research work, it was decided to tune controllers empirically based on the developed prototype. Due to tests carried out in a real environment, a more precise controller could be achieved. This approach requires a test platform that allows performing experiments safely. The main criterion is that the test bench must provide three degrees of rotational freedom, and the device under test must have the freedom to rotate around the yaw, pitch, and roll axis. Moreover, flying platform attachments to the test bench must be designed with an adjustable center of gravity.

The assembly is divided into four subassemblies: stationary support frame assembly, outer frame assembly, inner frame assembly, and attachment assembly. Stationary frame is a base assembly that provides support for others. The outer frame assembly is directly attached to it through a bearing, which provides rotation around the yaw axis. The inner frame assembly is attached to the outer frame assembly through two bearings to provide rotation around the roll axis. The final attachment assembly acts as a connecting link between the flying platform and the test bench, and it is connected to the inner frame through two bearings to provide rotational freedom for the pitch axis. The proposed gimbal-type frame with measurements and arc arrows showing rotating joints is presented in Fig. 8.



PID (proportional-integral-derivative) controllers are chosen to provide correction signals for stabilisation; to tune the controller, only orientation information is necessary. The sensor function uses Adafruit unified sensor library functions to obtain information from the sensor.

3.2. Testing and PID Tuning

Assessing the VTOL platform capabilities and the test bench suitability for the PID gain tuning is essential. Two tests were carried out to validate the developed solution: thrust map test and PID gain tuning using the heuristic tuning method. After completion of the tests, it is expected that the flight platform removed from the test bench will be ready for field testing.

The first test was carried out to map thrust of the motor using test equipment shown in Fig. 9a. Based on [17] and theoretical specifications of the individual EDFs, the constructed tandem EDF motor is expected to provide more than 3000 g of thrust. To validate expectations, test environment was constructed. For this purpose, scale with the measurement range of 0 to 5000 g and the tolerance of 1 g was used. Throttle signal was limited in each phase by mapping the corresponding variable in the algorithm. Pitch and roll servos were deactivated to ensure stability. Each test phase was dedicated to a certain throttle percentage. The throttle map in respect to thrust is shown in Fig. 9b.

The test revealed that the expectations were optimistic and the actual maximum thrust was approximately 2100 g. While thrust map function is nearly linear, it allows the

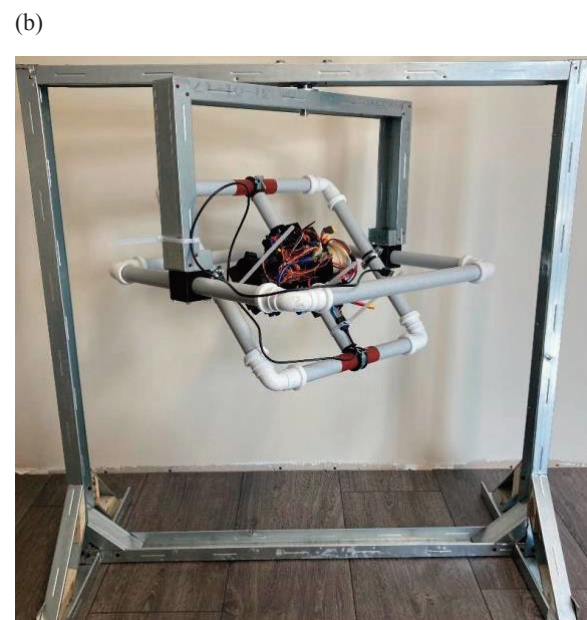


Fig. 8. Test bench assembly (a) and picture of a flying platform attached to the test bench (b).

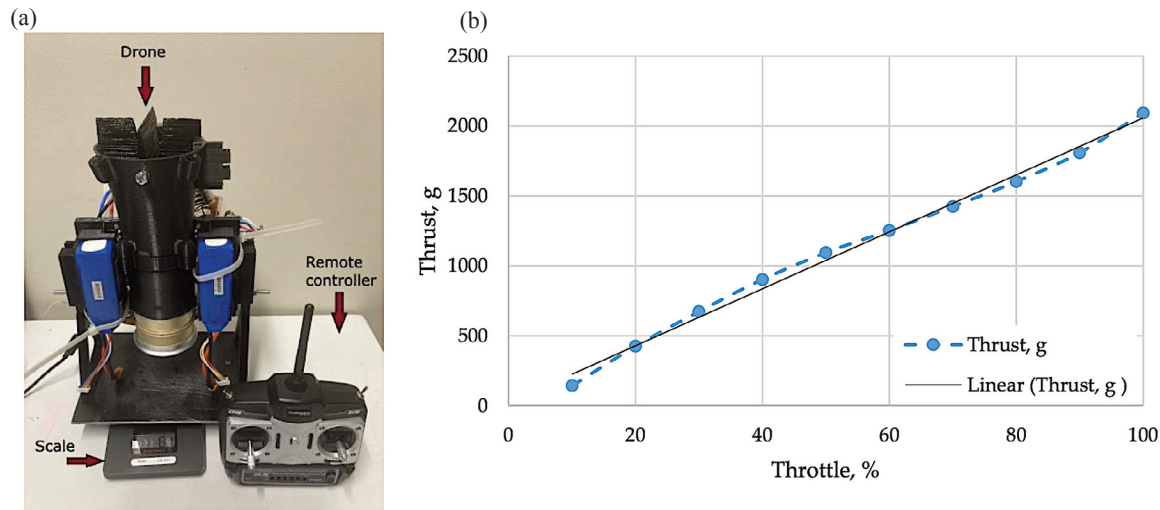


Fig. 9. Throttle mapping test equipment (a) and throttle map graph (b): blue dashed line – the actual test result, black – trendline.

implementation of separate PID controller gain parameters for each region. Such controller approach would give accurate and stable flight characteristics. PID equation gain parameters must be tuned to achieve a sufficient control algorithm performance. As a case study, gain parameters for 80% throttle were tuned. The tuning process for each axis controller was identical. This is expected to be sufficient (based on thrust map) to validate the proposed solution.

To evaluate the PID response performance, 60 degrees from setpoint disturbance was selected. A tuned PID response graph for roll controller response is shown in Fig. 10. It indicates a particularly large proportional gain parameter compared to the five dynamic behaviours (described above). Overall, the graph shows that the system stabilises eventually.

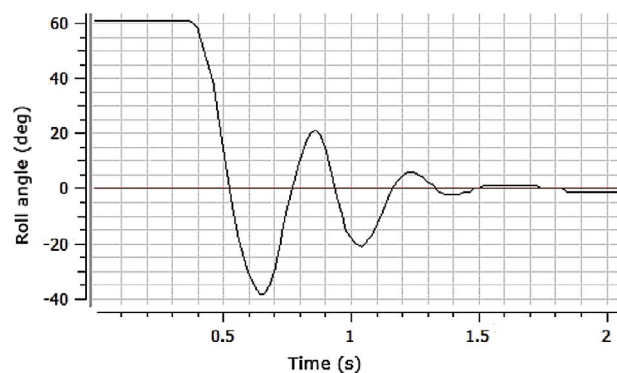


Fig. 10. Roll PID controller disturbance rejection graph, black line – actual position measured by the inertial sensor, red line – setpoint.

4. CONCLUSIONS

This research work seeks a solution for the tail-sitter VTOL automated hovering algorithm. The problem is that the existing solutions are multifunctional, trying to solve control logic for many different concepts. Despite the fact that some solutions are dedicated to a specific model, these solutions are highly theoretical and validated only by simulation. This leads to a loss in the performance and speed of the controller. However, the test bench with three degrees of freedom (3 DoF) for non-destructive testing and thrust force fixture mapping is developed.

The developed platform is a goal-focused robust, simple, and failproof control logic system for the tail-sitter VTOL. A VTOL drone with a tandem EDF motor is constructed and the control algorithm for testing the developed platform is presented. The PID controller tuning trials revealed that the proposed principle for controller tuning is simple and effective. It should be mentioned that the dynamic weight of the cable connecting the computer and the drone affects the dynamics of the model. Therefore, results differ for each iteration, and the final parameters cannot be achieved. After the cable connection improvement, further controller tuning must be performed. Overall, the trials validate that the actuator system and the algorithm are sufficient to control the process output behavior in the desired way, and the system can be stabilised with two PID controllers.

Future work on developing the tandem EDF motor tail-sitter VTOL drone prototype will focus on several key improvements. These include further optimisation of the flight platform actuator system, the wiring schematic, and the control system. The prototype's performance is also planned to be further enhanced by adapting metal ad-

ditively manufactured parts to replace the printed thermoplastics. Structural components, such as the chassis and mounts, will be printed from AlSi10Mg aluminum alloy, combining both light weight and excellent mechanical characteristics. The components will be printed in Tallinn University of Technology on the laser powder bed fusion (L-PBF) system SLM-280 by SLM Solutions Group AG. Prior to printing, the components will undergo topology optimisation procedures for overall weight reduction.

ACKNOWLEDGEMENTS

This research work was supported by the Estonian Ministry of Education and Research (Project PRG-1827). The publication costs of this article were covered by the Estonian Academy of Sciences.

APPENDIX

Disclaimers and acknowledgements of references

Research paper reference	Disclaimer(s)	Acknowledgement(s)
[17] – Tandem EDF engine	Only covers engine characteristics; not implemented on physical UAV.	Benefits and flaws of tandem EDF systems; design characteristics of tandem EDF systems.
[6,7] – Review of VTOL systems	Not dedicated to any tests or simulations; only analytical research.	Description of most VTOL concepts and most existing VTOL control methods.
[1–4] – Aerodynamics of conventional aircraft	N/A	Principles of aerodynamics.
[11] – Model-free or model-based design	Results are validated only in simulation.	Comparison of LRQ (linear quadratic regulator) and PID controller dedicated to tail-sitter; model-free design can give better results.
[20] – Control of tiltrotor UAV	Needs additional hardware to achieve its maximum performance	Robust control can achieve satisfactory results over full flight envelope.
[21,22] – Neural network control	VTOL: concept contributes only from one propeller.	Successful control methods based on neural network; results validated in simulation and real environment.
[12]	Not VTOL: results are validated only in simulation.	Possible control method for tandem EDF engine solution; dynamic model of axially placed tandem EDF engine.
[13–15]	VTOL: concept contributes only from one propeller; results are validated only in simulation.	Design and model of similar VTOL concept.
[16]	Not VTOL: EDF engines are not placed axially (concept is different); results are validated only in simulation.	Possible control method for tandem EDF fan solution; characteristics of tandem EDF engine.

REFERENCES

1. Federal Aviation Administration, U.S. Department of Transportation. *Instrument Flying Handbook (FAA-H-8083-15)*. 2001.
2. Federal Aviation Administration, U.S. Department of Transportation. *Helicopter Flying Handbook (FAA-H-8083-21B)*. 2019.
3. Rotaru, C. and Todorov, M. Helicopter flight physics. In *Flight Physics – Models, Techniques and Technologies* (Volkov, K., ed.). Kingston University, London, UK, 2018. <https://doi.org/10.5772/intechopen.71516>
4. Conlisk, A. T. Modern helicopter aerodynamics. *Annu. Rev. Fluid. Mech.*, 1997, **29**, 515–567. <https://doi.org/10.1146/annurev.fluid.29.1.515>
5. Allen, F. J. Bolt upright: Convair’s and Lockheed’s VTOL fighters. *Air Enthusiast* 2007, **127**. <https://portal.issn.org/resource/ISSN/0143-545>
6. Ducard, G. J. J. and Allenspach, M. Review of designs and flight control techniques of hybrid and convertible VTOL UAVs. *Aerosp. Sci. Technol.*, 2021, **118**, 107035. <https://doi.org/10.1016/J.AST.2021.107035>
7. Zhou, Y., Zhao, H. and Liu, Y. An evaluative review of the VTOL technologies for unmanned and manned aerial vehicles. *Comput. Commun.*, 2020, **149**, 356–369. <https://doi.org/10.1016/j.comcom.2019.10.016>
8. Li, B., Zhou, W., Sun, J., Wen, C. Y. and Chen, C. K. Development of model predictive controller for a tail-sitter VTOL UAV in hover flight. *Sensors*, 2018, **18**(9), 2859. <https://doi.org/10.3390/S18092859>

9. Cristillo, D., di Caprio, F., Pezzella, C., Paciello, C., Magistro, S., di Palma, L. et al. On numerical models for cube drop test of bladder fuel tank for aeronautical applications. *J. Compos. Sci.*, 2022, **6**(3), 99. <https://doi.org/10.3390/jcs6030099>
10. Zanotti, A. Experimental study of the aerodynamic interaction between side-by-side propellers in eVTOL airplane mode through stereoscopic particle image velocimetry. *Aerospace*, 2021, **8**(9), 239. <https://doi.org/10.3390/aerospace8090239>
11. Barth, J. M. O., Condomines, J. P., Bronz, M., Lustosa, L. R., Moschetta, J. M., Join, C. et al. Fixed-wing UAV with transitioning flight capabilities: model-based or model-free control approach? A preliminary study. In *Proceedings of the 2018 International Conference on Unmanned Aircraft Systems (ICUAS), Dallas, TX, USA, 12–15 June 2018*. IEEE, 1157–1164. <https://doi.org/10.1109/ICUAS.2018.8453404>
12. Bonci, A., Cervellieri, A., Longhi, S., Nabissi, G. and Scala, G. A. The Double Propeller Ducted-Fan, an UAV for safe Infrastructure inspection and human-interaction. In *Proceedings of the IEEE International Conference on Emerging Technologies and Factory Automation (ETFA), Vienna, Austria, 8–11 September 2020*. <https://doi.org/10.1109/ETFA46521.2020.9212035>
13. Marconi, L., Naldi, R. and Sala, A. Modeling and analysis of a reduced-complexity ducted MAV. In *Proceedings of the 14th Mediterranean Conference on Control and Automation (MED'06), Ancona, Italy, 28–30 June 2006*. IEEE, 2007, 9189104. <https://doi.org/10.1109/MED.2006.328770>
14. Naldi, R., Marconi, L. and Sala, A. Modelling and control of a miniature ducted-fan in fast forward flight. In *Proceedings of the American Control Conference, Seattle, WA, USA, 11–13 June 2008*. IEEE, 2552–2557. <https://doi.org/10.1109/ACC.2008.4586875>
15. Naldi, R., Gentili, L., Marconi, L. and Sala, A. Design and experimental validation of a nonlinear control law for a ducted-fan miniature aerial vehicle. *Control Eng. Pract.*, 2010, **18**(7), 747–760. <https://doi.org/10.1016/j.conengprac.2010.02.007>
16. Zhang, Y., Xiang, C., Xu, B., Wang, X. and Fan, W. Comprehensive nonlinear modeling and attitude control of a novel tandem ducted fan vehicle. In *Proceedings of the 2016 IEEE International Conference on Aircraft Utility Systems (AUS), Beijing, China, 10–12 October 2016*. IEEE, 50–56. <https://doi.org/10.1109/AUS.2016.7748019>
17. Lihulinn, M. *Construction of Tandem EDF Engine*. Estonian Aviation Academy, Tartu, 2018 (in Estonian).
18. Dr. Mad Thrust 70mm 10-Blade Alloy EDF 3000KV Motor – 1200W (4S) | HobbyKing. https://hobbyking.com/en_us/dr-mad-thrust-70mm-10-blade-alloy-edf-3000kv-motor-1200w-4s.html (accessed 2022-07-05).
19. Pütsep, K., Rassõlkin, A. and Vaimann, T. Conceptual test bench for small class unmanned autonomous vehicle performance estimation. In *Proceedings of the IEEE 19th International Power Electronics and Motion Control Conference (PEMC), Gliwice, Poland, 25–29 April 2021*. IEEE (Accepted for publication).
20. Liu, Z., He, Y., Yang, L. and Han, J. Control techniques of tilt rotor unmanned aerial vehicle systems: a review. *Chinese J. Aeronaut.*, 2017, **30**(1), 135–148. <https://doi.org/10.1016/j.cja.2016.11.001>
21. Cheng, Z., Pei, H. and Li, S. Neural-networks control for hover to high-speed-level-flight transition of ducted fan UAV with provable stability. *IEEE Access*, 2020, **8**, 100135–100151. <https://doi.org/10.1109/access.2020.2997877>
22. Xu, J., Du, T., Foshey, M., Li, B., Zhu, B., Schulz, A. et al. Learning to fly: computational controller design for hybrid UAVs with reinforcement learning. *ACM Trans. Graph.*, 2019, **38**(4), 1–12. <https://doi.org/10.1145/3306346.3322940>

Vertikaalselt startiva ja maanduva tandem-EDF mootoriga õhusõiduki arendamine ning katsetamine

Kristjan Pütsep, Tõivo Nerep, Hans Tiismus ja Anton Rassõlkin

Juhtimismehhanismide keerukuse tõttu ei ole vertikaalselt startivad ja maanduvad (*vertical take-off and landing*, VTOL) õhusõidukid leidnud laialdast kasutust. Tänu tehnoloogiale arengule ja kättesaadavusele on võimalik kasutada ka lihtsaimaid süsteeme. Neid saaks rakendada transpordis, sõjanduses, järelevalves jm. Uurimistöö eesmärk on pakkuda välja automaatse stabiliseerimisjuhtimise algoritmi lahendus VTOL-i hõljumislennu faasi jaoks. Analüüsitakse olemasolevaid sarnase teemaga seotud uurimusi ning töötatakse välja ja esitletakse lennuplatvormi ning sobivat katsestendi mittepurustavateks testimisteks.

Lennuplatvormi ajamite süsteem koosneb kahest vastassuunas pöörlevast elektrilise tiiviku (*electrical ducted fan*, EDF) tõukemootoriga ja kahest servosüsteemist, mis kontrollivad piki- ja külgsuunalist stabiilsust. Artiklis kirjeldatakse juhtimisalgoritmi väljatöötamist, struktuuri ja katseid, mis kinnitavad väljapakutud lahendusi. Uurimistöö tulemused annavad kindla aluse VTOL-õhusõiduki arendamiseks ning katsestendi prototüüp demonstreerib kontseptsiooni, mida saab edaspidi kasutada erinevatel lennuplatvormidel.